

# Current induced magnetization dynamics and magnetization switching in superconducting ferromagnetic hybrid (F|S|F) structures

Saumen Acharjee\* and Umananda Dev Goswami†

*Department of Physics, Dibrugarh University, Dibrugarh 786 004, Assam, India*

We investigate the current induced magnetization dynamics and magnetization switching in an unconventional p-wave superconductor sandwiched between two misaligned ferromagnetic layers by numerically solving Landau-Lifshitz-Gilbert equation modified with current induced Slonczewski's spin torque term. A modified form of Ginzburg-Landau free energy functional has been used for this purpose. We demonstrated the possibility of current induced magnetization switching in the spin-triplet ferromagnetic superconducting hybrid structures with strong easy axis anisotropy and the condition for magnetization reversal. The switching time for such arrangement is calculated and is found to be highly dependent on the magnetic configuration along with the biasing current. This study would be useful in designing practical superconducting-spintronic devices.

PACS numbers: 67.30.hj, 85.75.-d, 74.90.+n

## I. INTRODUCTION

During over last 15 years, a number of very interesting compounds have been discovered which reveal the coexistence of ferromagnetism and superconductivity in the same domain in bulk [1–6]. The interplay between ferromagnetic order and superconductivity thus gains lots of attention from variety of research communities [7]. Among those, some people were hunting for superconductivity in a ferromagnetic spin valve made up of two ferromagnetic substances separated by a superconducting element (F|S|F system). In this context it is to be noted that, the spin triplet superconductivity in superconductor|ferromagnet (F|S) hybrid structures including F|S|F spin valves is a topic of intense research [8–16] in the theoretical as well as experimental points of view for almost last two decades. The major interest of the F|S hybrid structures is due to the dissipation less flow of charge carriers offered by the superconducting environment. To completely understand this hybrid structure it is important to study the spin polarized transport.

Moreover, the transport of spin is closely related to the phenomenon of current induced magnetization dynamics [17] and spin transfer torque [18, 19]. Spin transfer torque (STT), which is the building block of spintronics is based on the principle that, when a spin polarized current is applied into the ferromagnetic layers, spin angular momentum is transferred into the magnetic order. It is observed that for a sufficiently large current, magnetization switching can occur [20, 21] in a magnetic layer. Thus, the flow of electrons can be served to manipulate the configuration of the spin valves. Traditionally, a lot of works had been done earlier on current induced magnetization dynamics and STT on ferromagnetic layers. Soon after, a lot attention have been made on anti-ferromagnetic layers [21–24] also. Making a hybrid structure of a superconductor with a ferromagnet and the concept of current induced magnetization dynamics suggest a very interesting venue for

combining two different fields, namely superconductivity and spintronics [25]. A few works had been done earlier on F|S hybrid structures [26–30]. In Ref. [20], supercurrent-induced magnetization dynamics in Josephson junction with two misaligned ferromagnetic layers had been studied and demonstrated the favourable condition for magnetization switching and reversal.

Motivated by the earlier works, in this paper we studied the current induced magnetization dynamics of a superconducting ferromagnet in a hybrid structure of F|S based on Landau-Lifshitz-Gilbert (LLG) equation with Slonczewski's torque (LLGS) using the Ginzburg-Landau-Gibb's free energy functional. The proposed experimental setup is shown in the Fig.1, in which two ferromagnets are separated by a thin superconducting ferromagnet. The coercive fields of the ferromagnets are such that, the magnetization is hard in one layer while soft in the other and the orientation of magnetization of the soft ferromagnetic layer is supposed to be misaligned with the hard ferromagnetic layers by an angle  $\theta$ . When the junction is current-biased, it gets spin polarized in the hard layer and thus transfer angular momentum to the magnetic order. This generates an induced magnetization contributing to the magnetic order. The dynamics of this induced magnetization has been studied by numerically solving the LLGS equation.

The paper is organized as follows. In the Section II, a theoretical framework of the proposed setup is developed. The results of our work is discussed in the Section III by solving LLGS equation numerically. Finally we conclude our work in the Section IV.

## II. THEORY

To study the current induced magnetization dynamics of a ferromagnetic superconductor with easy axis anisotropy in F|S|F spin valve, we utilized Landau-Lifshitz-Gilbert (LLG) equation with the Slonczewski's spin transfer torque (LLGS). The resulting LLGS equation takes the form

$$\frac{\partial \mathbf{M}}{\partial t} = -\gamma(\mathbf{M} \times \mathbf{H}_{eff}) + \alpha(\mathbf{M} \times \frac{\partial \mathbf{M}}{\partial t}) + \mathbf{T}, \quad (1)$$

\*saumenacharjee@gmail.com

†umananda2@gmail.com

where  $\gamma$  is the gyromagnetic ratio,  $\alpha$  is the Gilbert's damping constant and  $H_{eff}$  is the effective magnetic field of superconducting ferromagnet.  $\mathbf{T}$  is the current induced spin transfer torque and can be read as [20]

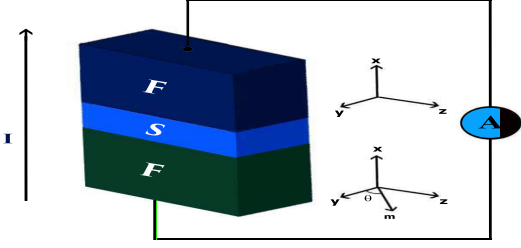


FIG. 1: The proposed experimental setup. An unconventional p-wave type superconductor is sandwiched in between two ferromagnetic layers. The magnetization orientation of the ferromagnetic layers are supposed to be misaligned by an angle  $\theta$ . When a current  $I$  is injected it gets polarized and transfer of spin torque to the magnetic order causing magnetization dynamics. Different colours of the ferromagnetic layers indicates the level of magnetization. Here, the bottom layer is hard in magnetization.

$$\mathbf{T} = I\zeta(\mathbf{M} \times [\mathbf{M} \times (\mathbf{M}_T - \epsilon\mathbf{M}_B)]), \quad (2)$$

where  $\mathbf{M}_T$  and  $\mathbf{M}_B$  respectively represents the normalized magnetization vector in the top and bottom magnetic layers of the spin valve and is taken as  $\mathbf{M}_T = (0, 1, 0)$  and  $\mathbf{M}_B = (0, \cos \theta, \sin \theta)$  such that for  $\theta = 0$ , the configuration is parallel and is anti-parallel for  $\theta = \pi$ .  $\epsilon$  provides the factor of asymmetry in polarization in top and bottom ferromagnetic layers. The term  $\zeta$  is given by

$$\zeta = \frac{\nu\hbar\mu_0}{2em_0V}. \quad (3)$$

Here,  $e$  is the electronic charge,  $\nu$  is the polarization efficiency,  $\hbar$  is the Planck's constant,  $\mu_0$  is the magnetic permeability,  $m_0$  is the amplitude of magnetization and  $V$  is the volume of the system.  $I$  is the applied current bias. The effective magnetic field of the system can be obtained from the functional derivative of the free energy with respect to the magnetization:

$$\mathbf{H}_{eff} = -\frac{dF}{d\mathbf{M}}. \quad (4)$$

The free energy functional  $F(\psi, \mathbf{M})$  can be given by [31]

$$F(\psi, \mathbf{M}) = \int d^3\mathbf{r} f(\psi, \mathbf{M}), \quad (5)$$

where  $f(\psi, \mathbf{M})$  gives the free energy density of a spin-triplet superconductor and can be read as [31, 32]

$$f(\psi, \mathbf{M}) = f_S(\psi) + f_F(\mathbf{M}) + f_{int}(\psi, \mathbf{M}) + \frac{\mathbf{B}^2}{8\pi} - \mathbf{B} \cdot \mathbf{M}, \quad (6)$$

where  $\psi (\equiv \psi_j; j = 1, 2, 3)$  is the superconducting order parameter and is a three dimensional complex vector,  $\mathbf{M}$  is the magnetization vector, which characterizes the ferromagnetism,  $f_S(\psi)$  gives the superconductivity, while the ferromagnetic order is described by  $f_F(\mathbf{M})$ . The interaction of the two orders,  $\mathbf{M}$  and  $\psi$  is described by the term  $f_{int}(\psi, \mathbf{M})$ . The last two terms in equation (6) account the contribution of magnetic energy on free energy with magnetic induction  $\mathbf{B} = \mathbf{H} + 4\pi\mathbf{M} = \nabla \times \mathbf{A}$ .

The superconductivity of the system is described by the term  $f_S(\psi)$  under the condition  $\mathbf{H} = 0$  and  $\mathbf{M} = 0$  and can be written as [31–33]

$$f_S(\psi) = f_{grad}(\psi) + a_s|\psi|^2 + \frac{b_s}{2}|\psi|^4 + \frac{u_s}{2}|\psi^2|^2 + \frac{v_s}{2} \sum_{i=1}^3 |\psi|^4, \quad (7)$$

where  $f_{grad}$  can be written as [32]

$$f_{grad} = K_1(D_i\psi_j)^*(D_i\psi_j) + K_2[(D_i\psi_i)^*(D_j\psi_j) + (D_i\psi_j)^*(D_j\psi_i)] + K_3(D_i\psi_i)^*(D_i\psi_i) \quad (8)$$

with  $D_i = -i\hbar(\frac{\partial}{\partial x_i}) + 2\frac{|e|}{c}A_i$  being the covariant derivative,  $u_s$  describes the anisotropy of the spin triplet Cooper pair and the crystal anisotropy is described by  $v_s$ .  $a_s$  and  $b_s$  are positive material parameters. The term  $f_F(\mathbf{M})$  in (6) describes the ferromagnetic ordering of the material and is given by [31, 32]

$$f_F(\mathbf{M}) = c_f \sum_{j=1}^3 |\nabla_j \mathbf{M}_j|^2 + a_f \mathbf{M}^2 + \frac{b_f}{2} \mathbf{M}^4. \quad (9)$$

While the term  $f_{int}(\psi, \mathbf{M})$  in (6) corresponds to the interaction of ferromagnetic order with the complex superconducting order and can be written as

$$f_{int}(\psi, \mathbf{M}) = i\gamma_0 \mathbf{M} \cdot (\psi \times \psi^*) + \delta \mathbf{M}^2 |\psi|^2, \quad (10)$$

where  $\gamma_0$  term provides the superconductivity due to ferromagnetic order, while  $\delta$  term makes the model more realistic as it represent the strong coupling and can be both positive and negative values. Rewriting the free energy  $f(\psi, \mathbf{M})$  in a dimensionless form by redefining the order parameters  $\psi_j = b_s^{-\frac{1}{4}} \phi_j e^{i\theta_j}$  and  $\mathbf{m} = b_f^{-\frac{1}{4}} \mathbf{M}$ , the free energy (6) takes the form

$$f = f_{grad} + r\phi^2 + \frac{1}{2}\phi^4 - 2t_1[\phi_1^2\phi_2^2\sin^2(\theta_2 - \theta_1) + \phi_1^2\phi_3^2\sin^2(\theta_1 - \theta_3) + \phi_2^2\phi_3^2\sin^2(\theta_2 - \theta_3)] - v[\phi_1^2\phi_2^2 + \phi_2^2\phi_3^2 + \phi_3^2\phi_1^2] + w\mathbf{m}^2 + \frac{1}{2}\mathbf{m}^4 + 2\gamma_1\phi_1\phi_3\mathbf{m}\sin(\theta_3 - \theta_1) + \gamma_2\phi^2\mathbf{m}^2 - v_1\mathbf{B} \cdot \mathbf{m}, \quad (11)$$

where the parameters,  $r = \frac{a_s}{b_s^{\frac{1}{2}}}$ ,  $w = \frac{a_f}{b_f^{\frac{1}{2}}}$ ,  $t_1 = \frac{u_s}{b}$ ,  $v = \frac{v_s}{b}$ ,

$$\gamma_1 = \frac{\gamma_0}{b^{\frac{1}{2}}b_f^{\frac{1}{4}}}, \gamma_2 = \frac{\delta}{(bb_f)^{\frac{1}{2}}} \text{ and } v_1 = b_f^{\frac{1}{4}} \text{ with } b = (b_s + u_s + v_s).$$

The coexistence of superconductivity and ferromagnetism was first observed in UGe<sub>2</sub> [1, 34] within a limited pressure range (1.0 - 1.6 GPa). In following years, same coexistence was found in URhGe [2, 34] and UCoGe [4, 34, 35] at ambient pressure, and in UIr [36] similar to the case of UGe<sub>2</sub>, i.e. within a limited pressure range (2.6 - 2.7 GPa). These Uranium-based (U-based) compounds, with the coexistence of ferromagnetism and superconductivity, exhibit unconventional properties of ground state in a strongly correlated ferromagnetic system. One of the interesting features of these U-based ferromagnetic superconductors is that, this type of superconductivity was found to occur within the vicinity of a quantum critical point (QCP). The critical pressure, or critical chemical composition is referred to as the QCP, where the ordering temperature is tuned to  $T_C = 0$  K. It should be noted that in general, the U-based ferromagnetic superconductors have a very strong easy-axis magneto crystalline anisotropy [31, 34]. However, the free energy in equation (11) is isotropic. To account the contribution of anisotropy in free energy, we introduce a term  $K_{an}$  [20] resulting in an effective field of the form  $H_{an} = (K_{an}m_y/M_0)\hat{y}$ . Here we direct the anisotropy axis in parallel to the y-direction and contribution along the anisotropy axis is being considered. In view of this, the LLGS equation (1) takes the form

$$\frac{\partial \mathbf{m}}{\partial t} = -\gamma[\mathbf{m} \times (2w\mathbf{m} + 2\mathbf{m}^3 + 2\gamma_1\phi_1\phi_3\sin(\theta_3 - \theta_1)\hat{y} + 2\gamma_2\phi^2\mathbf{m} - v_1\mathbf{B} + \frac{K_{an}m_y}{M_0}\hat{y})] + \alpha(\mathbf{m} \times \frac{\partial \mathbf{m}}{\partial t}) + \mathbf{T}, \quad (12)$$

where  $\mathbf{m}_y$  is the component of  $\mathbf{m}$  along the anisotropy axis which we direct parallel to y-axis with  $\mathbf{B} = -B_0\hat{z}$ . The equation (12) is a non-linear coupled differential equation in  $\mathbf{m}$  and can be transformed into the following form

$$\begin{aligned} \frac{dm_x}{d\tau} = & \alpha\epsilon I \sin \theta m_y^3(\tau) + \alpha I(1 - \epsilon \cos \theta)m_y^2(\tau)m_z(\tau) \\ & + \alpha I(1 - \epsilon \cos \theta)m_z^3(\tau) + \alpha I m_x^2(\tau)[\epsilon \sin \theta m_y(\tau) \\ & + (1 - \epsilon \cos \theta)m_z(\tau)] + m_y(\tau)[-B_0v_1 + m_z(\tau)(K_{an} \\ & + 2w + \alpha\epsilon I \sin \theta m_z(\tau) + 2\phi^2\gamma_2)] + 2 \sin \beta m_z(\tau)\gamma_1\phi_1\phi_3 \\ & - m_x(\tau)[m_z(\tau)(\epsilon I \sin \theta + \alpha B_0v_1) + \alpha m_y^2(\tau)(K_{an} + 2w \\ & + 2\phi^2\gamma_2) + m_y(\tau)(-I + \epsilon I \cos \theta + 2\alpha\gamma_1\phi_1\phi_3 \sin \beta)] \\ & / [1 + \alpha^2(m_x^2(\tau) + m_y^2(\tau) + m_z^2(\tau))], \quad (13) \end{aligned}$$

$$\begin{aligned} \frac{dm_y}{d\tau} = & -\alpha\epsilon I \sin \theta m_x^3(\tau) + m_x(\tau)[- \alpha\epsilon I \sin \theta(m_x^2(\tau) \\ & + m_z^2(\tau)) + B_0v_1] + m_x^2(\tau)[-I + \epsilon I \cos \theta + \alpha m_y(\tau)(K_{an} \\ & + 2w + 2\phi^2\gamma_2) + 2\alpha \sin \beta \gamma_1\phi_1\phi_3] + m_z(\tau)[m_y(\tau)(-\epsilon I \sin \theta \\ & - \alpha B_0v_1 + \alpha m_z(\tau)(K_{an} + 2w + 2\phi^2\gamma_2)) + m_z(\tau)(I(-1 \\ & + \epsilon \cos \theta) + 2\alpha \sin \beta \gamma_1\phi_1\phi_3)] / [1 + \alpha^2(m_x^2(\tau) \\ & + m_y^2(\tau) + m_z^2(\tau))], \quad (14) \end{aligned}$$

$$\begin{aligned} \frac{dm_z}{d\tau} = & \alpha I(1 + \epsilon \cos \theta)m_x^3(\tau) + m_x^2(\tau)(I\epsilon \sin \theta + \alpha B_0v_1) \\ & - m_x(\tau)[\alpha I(1 - \epsilon \cos \theta)m_y^2(\tau) + \alpha I(1 - \epsilon \cos \theta)m_z^2(\tau) \\ & + m_y(\tau)(K_{an} + 2w + 2\phi^2\gamma_2) + 2 \sin \beta \gamma_1\phi_1\phi_3] \\ & + m_y(\tau)[m_y(\tau)(\epsilon I \sin \theta + \alpha B_0v_1 - \alpha m_z(\tau)(K_{an} + 2w \\ & + 2\phi^2\gamma_2)) + m_z(\tau)(I - \epsilon I \cos \theta - 2\alpha \sin \beta \gamma_1\phi_1\phi_3)] \\ & / [1 + \alpha^2(m_x^2(\tau) + m_y^2(\tau) + m_z^2(\tau))], \quad (15) \end{aligned}$$

where  $\beta = (\theta_3 - \theta_1)$  represents the phase mismatch of surviving components of the superconducting order parameter. For a realistic situation this phase mismatch should not be very large and hence we have taken the  $\beta$  to be equal to  $0.1\pi$  arbitrarily to have a similarity with the practical situation. As U-based ferromagnetic superconductors have a very strong magneto crystalline anisotropy [31, 34], to model a realistic superconducting ferromagnet, the anisotropy field can be taken as [34]  $K_{an} \sim 10^3$ , the asymmetry factor is taken as  $\epsilon = 0.1$  with magnetic induction  $B_0 = 0.1$  and  $\zeta = 1$ . Furthermore, we have set [31]  $v_1 = w = 0.1$ ,  $\phi_1 = \phi_3 = \frac{\phi}{\sqrt{2}}$  and initially  $\gamma_1 = 2\gamma_2 = 0.2$ , which make F|S|F spin valve system more realizable.

### III. RESULTS AND DISCUSSIONS

To investigate the magnetization dynamics and switching behaviour quantitatively, we have solved the full LLGS equations (13, 14, 15) of the F|S|F system using numerical simulation. The magnetization dynamics and switching behaviour of our system are investigated based on the above mentioned parameters, initially for very weak damping ( $\alpha \ll 1$ ) and then for strong damping (up to  $\alpha = 0.5$ ) with a very small angle of misalignment  $\theta = 0.1\pi$  and  $\gamma_1 = 2\gamma_2 = 0.2$ . Furthermore, to solve the equations (13, 14, 15) numerically the time coordinate has been normalized to  $\tau = \gamma t/M_0$ , where  $M_0$  is the magnitude of the magnetization. Few of the corresponding numerical solutions are shown in Fig.2 for two different current biasing in the first four plots. The rest plots in the figure show the corresponding parametric graphs of the time evolution of the magnetization components. The plots in left panels show the weak damping regime with Gilbert's damping parameter  $\alpha = 0.05$  for two different choices of current biasing 0.1 mA and 0.252 mA respectively from top to bottom. While the damping is considered to be strong with  $\alpha = 0.5$  in the plots of the right panels for the respective current biasings. It is seen that, the magnetization components show quite different behaviours. The components  $m_x$  and  $m_z$  display oscillating decay until they vanish completely, while on the other hand the component  $m_y$  saturates with the increasing value of  $\tau$ . It is to be noted that, the qualitative behaviour of the components of magnetization is similar for different damping parameters. But the quantitative difference is that, in strong Gilbert's damping regime, the oscillation of the magnetization components  $m_x$  and  $m_y$  die out faster in time scale, while the component  $m_z$  saturates too rapidly as seen from the right panels of Fig.2. It is also seen that in strong damping, the reversal of magnetization components  $m_y$  and  $m_z$  does

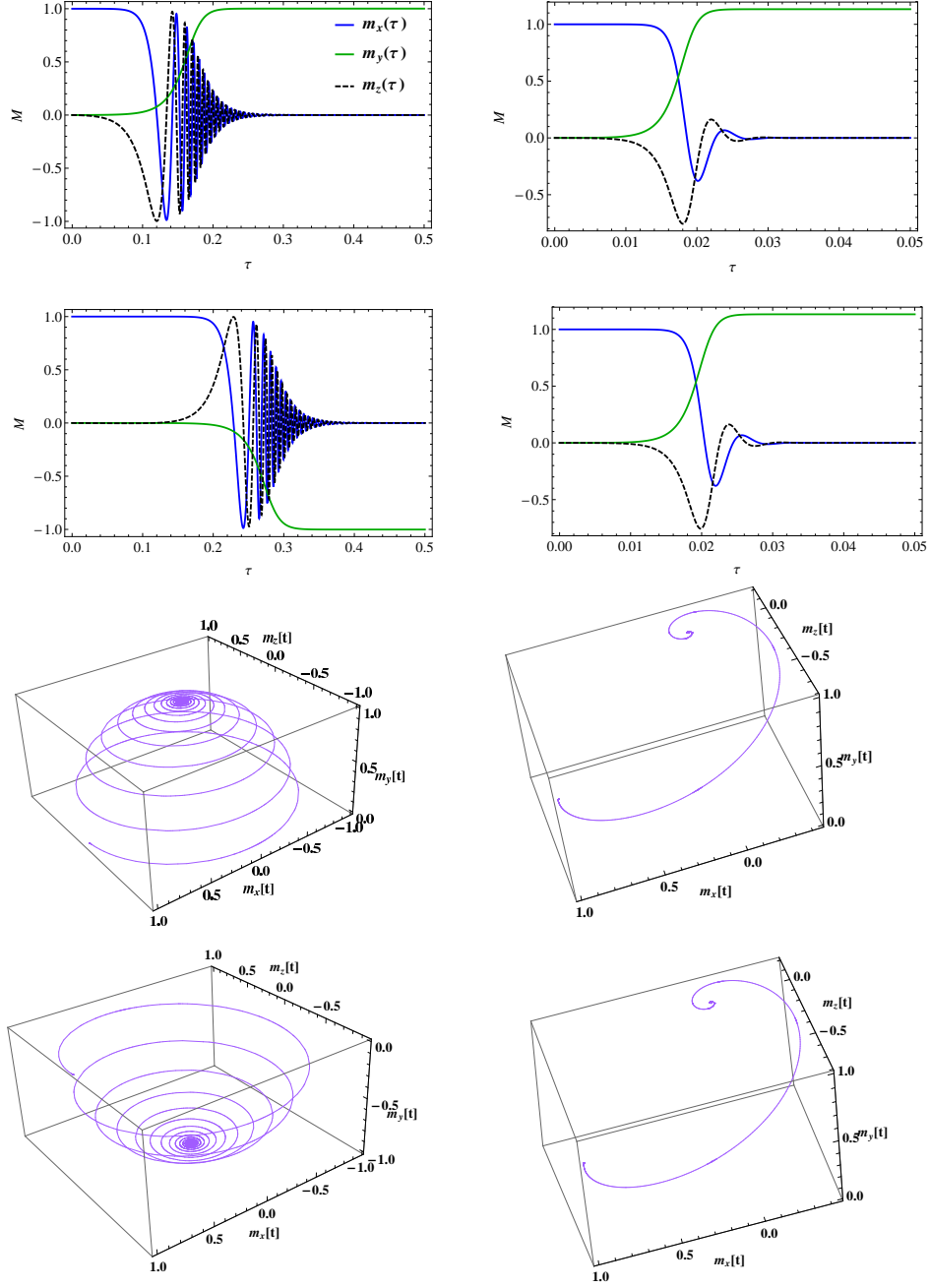


FIG. 2: (First four plots) The time evolution of the normalized components of magnetization with initial angle of misalignment  $\theta = 0.1\pi$  and with  $\gamma_1 = 2\gamma_2 = 0.2$ . The plots in the left panels depicted for the weak damping  $\alpha = 0.05$ , while the plots in the right panels are for strong damping  $\alpha = 0.5$  with a current biasing of 0.1 mA and 0.252 mA respectively from top to bottom panels. The corresponding parametric graphs representing the behaviour of the magnetization are displayed in the last four plots.

not occur for a current biasing  $I = 0.252$  mA, contrary to the case for the small damping. This result indicates that, it is possible to generate current induced magnetization reversal of a triplet superconducting ferromagnet in a F|S|F spin valve setup shown in Fig.1 by means of current biasing under weak damping condition.

It is also our interest to see what happens when the parameter  $\gamma_2$  is increased. To check the influence of  $\gamma_2$  on switching

mechanism, we investigated the behaviour of the magnetization components for both positive and negative values of  $\gamma_2$  keeping the damping parameter and  $\gamma_1$  fixed for currents respectively of  $I = 0.25$  mA and 0.252 mA. It is found that the switching time  $\tau$  gets delayed for  $\gamma_2 = -45$ , while on the other hand we observed a more rapid switching for  $\gamma_2 = 45$ . Moreover, the  $x$  and  $y$  components show more rapid oscillation for  $\gamma_2 = 45$  than for  $\gamma_2 = -45$ . The components of

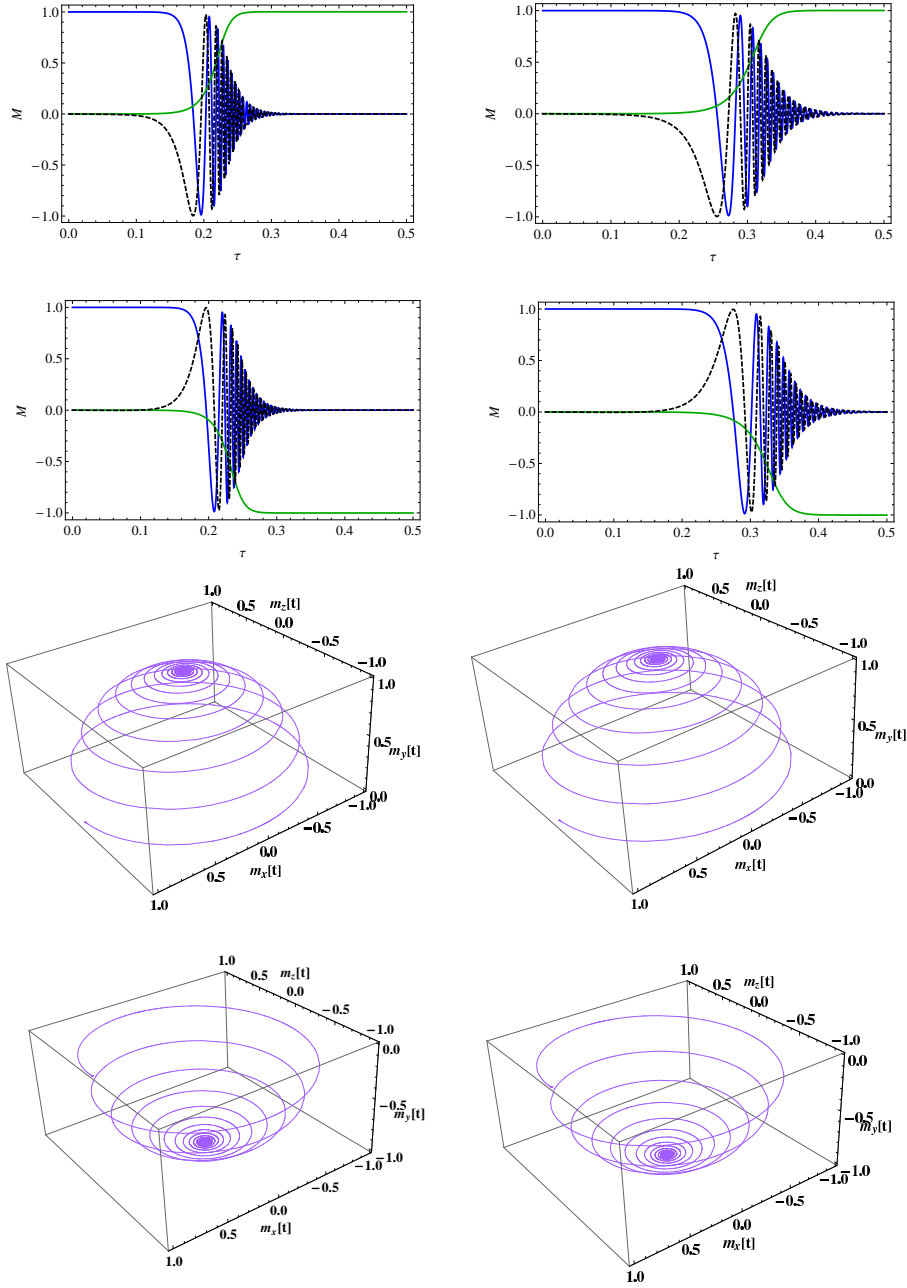


FIG. 3: (First four plots) The time evolution of the normalized components of magnetization with initial angle of misalignment  $\theta = 0.1\pi$ . Here  $\gamma_1 = 0.2$  with  $\gamma_2 = 45$  and  $-45$  respectively in left and right for current biasing  $I = 0.25$  mA in the top panels and  $0.252$  mA for the bottom panels keeping  $B_0 = 0.1$  constant. The corresponding parametric graphs representing the behaviour of the magnetization are shown in the last four plots.

magnetization under this condition are shown in Fig.3 with the parametric graphs. This result suggests that magnetization reversal is dependent on strong coupling parameter and the switching of a system is more rapid for positive coupling than that for negative coupling parameter as seen.

Our one more interest here is to check the influence of  $B_0$  on switching. To investigate this we have plotted the magnetization components for a higher value of  $B_0 = 1.0$  in Fig.4. It is seen that under this situation the switching does not even

occurs for a current biasing of  $1.5$  mA as seen from the middle panel. In this configuration the reversal of the magnetization components occurs at a current biasing of  $1.65$  mA as seen from right panel of Fig.4. This suggests that the magnetization switching condition can also be controlled by magnetic induction.

It is to be noted from the Fig.2 and Fig.3 that for the weak damping but with higher current biasing, oscillations and switching for reversal of respective components of mag-



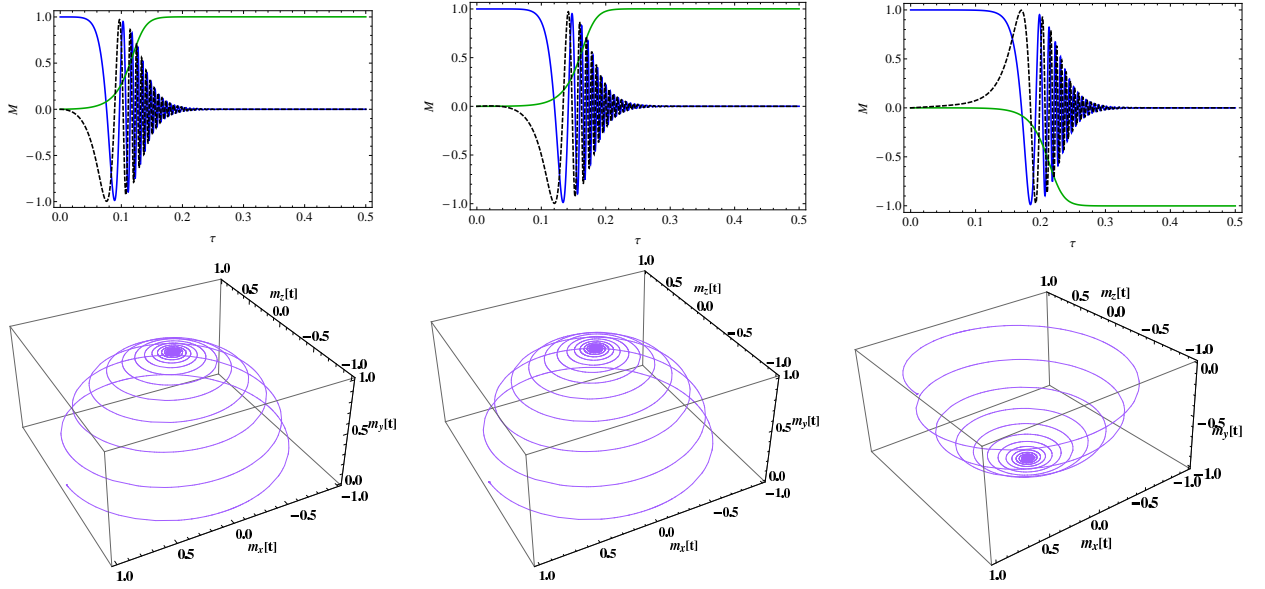


FIG. 4: (Top three plots) The time evolution of the normalized components of magnetization with initial angle of misalignment  $\theta = 0.1\pi$  for a magnetic induction  $B_0 = 1.0$  with  $\gamma_1 = 2\gamma_2 = 0.2$  and for weak damping  $\alpha = 0.05$ . The plots in left and right depicted the magnetization dynamics for a current biasing of 0.1 mA and 1.65 mA respectively, while the plot in the middle is for a current biasing of 1.5 mA. The corresponding parametric graphs representing the behaviour of the magnetization are shown in the bottom three plots.

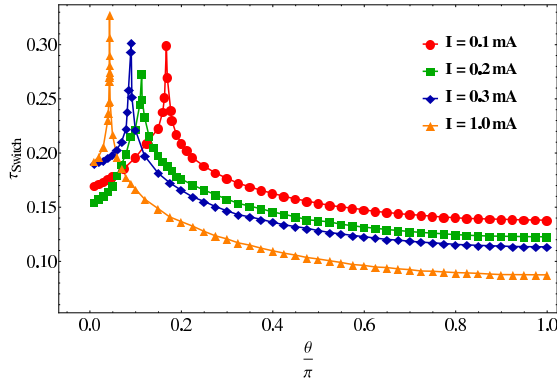


FIG. 5: Switching time and its dependence on the spin valve configuration for different current biasings.

netization are delayed by some factors. In view of this result, it is also important to see explicitly what happens to the spin valve if configuration is changed and what influence the spin valve configuration has on the switching time  $\tau_{switch}$ ?

To answer these two questions, we have studied the switching time  $\tau_{switch}$  as a function of  $\theta$  representing the angles of misalignments for four different current biasings keeping the damping factor  $\alpha = 0.05$  as shown in the Fig.5. It should be noted that, the switching time of a magnetization component is defined as the time required by the component to attain numerically the 0.975 times of its saturated value [21]. One of the important results of this study is that, for the increasing angle of misalignment, more rapid switching of corresponding components of magnetization occurs with the increasing value of the current bias. From the Fig.5 it is also seen that, for all

current biasing the switching time shows monotonic increase with a sharp peak starting from the zero angle of misalignment, providing the most delayed magnetic spin valve configuration at a particular current. The angle of misalignment of this most delayed configuration decreases with increasing value of the biasing current. It is interesting to note that, the maximum switching time for a particular angle of misalignment increases with increasing value of current biasing except for the case of 0.2 mA current, at which it is lowest. This particular behaviour at 0.2 mA current indicates that in the range of smaller angle of misalignment ( $\theta \leq 0.05\pi$ ), 0.2 mA is the optimum value of biasing current among all for the magnetic spin valve. The data of these results are summarized in Table I. These results as a whole clearly signify that, switching is highly dependent on magnetic configuration in association with the biasing current: switching occurs swiftly at higher angle of misalignment with higher value of current bias. This suggests that, the configuration near the anti-parallel ( $\theta = \pi$ ) offers rapid switching then the parallel ( $\theta = 0$ ) for all the current biasing, and for higher current, the peak position shifted towards the parallel configuration lowering the switching time just after the peak. This is quite obvious as the STT becomes stronger in this case.

Our final interest is to study the influence of higher magnetic field on the component of magnetization. To analyze this we have plotted the magnetization components with  $\tau$  for higher values of the magnetic field in Fig.6, keeping the biased currents fixed at 0.1 mA and  $\gamma_1 = 2\gamma_2 = 0.2$ . It is seen that for  $B_0 = 10^2$ , the components of magnetization shows quite similar behaviour as seen earlier in Fig.2. However, on the

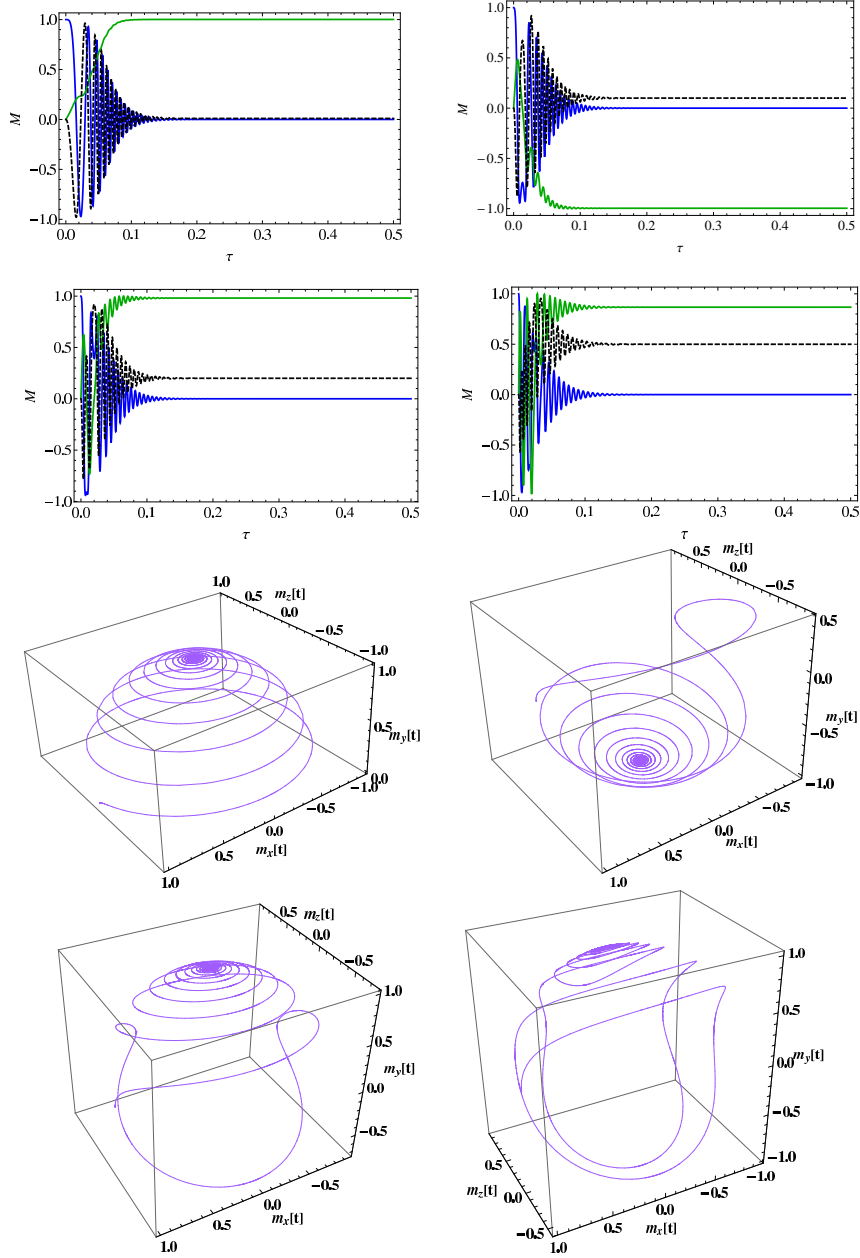


FIG. 6: (First four plots) The time evolution of normalized components of magnetization with initial angle of misalignment  $\theta = 0.1\pi$  with  $\gamma_1 = 2\gamma_2 = 0.2$  and for current biasing  $I = 0.1$  mA for higher values of external magnetic field, viz.,  $B_0 = 10^2$  (top left),  $B_0 = 10^3$  (top right),  $B_0 = 2 \times 10^3$  (bottom left) and  $B_0 = 5 \times 10^3$  (bottom right). The corresponding parametric graphs representing the behaviour of the magnetization are shown in the last four plots.

other hand as the magnetic field increases the components of magnetization shows quite irregular behaviour. For example, for  $B_0 = 10^3$  as seen from the top right panel of the Fig.6, the  $m_y$  component suddenly reverses with a small initial fluctuations and then starts saturating after a oscillating decay period. This is due to the fact that, as  $B_0$  becomes of the order of the anisotropy field, the components of magnetization behave quite differently. In this condition, the component  $m_y$  reverses and saturates, while  $m_x$  and  $m_z$  show an oscillating decay. With further rise in  $B_0$  makes the system more un-

stable in such a way that, with increasing value of  $B_0$ , both  $m_y$  and  $m_z$  components gradually tend to behave almost similarly by retaining the original direction of the  $m_y$  component as seen from the bottom panels of the first four plots in the Fig.6. Because, with further rise in  $B_0$ , the magnetic field dominates over the anisotropy field. It can be easily visualized from the parametric graph shown in the bottom left of panel of the Fig.6, where the motion takes place about the direction of magnetic field. The motion stabilizes itself for more higher values of  $B_0$ . We have found that, the influence of magnetic

TABLE I: Maximum switching time ( $\tau_{switch}$ ) and corresponding misalignment angle ( $\theta$ ) for different biasing currents in low damping with  $\alpha = 0.05$ .

I (in mA)	$\theta$	$\tau_{switch}$ (in Sec)
0.1	$0.168\pi$	0.2995
0.2	$0.114\pi$	0.2734
0.3	$0.091\pi$	0.3022
1.0	$0.044\pi$	0.3280

field as mentioned above is almost similar for the biasing current and hence higher value of magnetic field ( $B_0 \geq 100$ ) eliminates the effect of biasing current.

#### IV. SUMMARY

In this work, we have investigated the current induced magnetization dynamics and magnetization switching in a superconducting ferromagnet sandwiched between two misaligned ferromagnetic layers with easy-axis anisotropy by numerically solving Landau-Lifshitz-Gilbert-Slonczewski's equation. For this purpose, we have used the modified form of the Ginzburg-Landau free energy functional for a triplet p-wave superconductor. We have demonstrated about the possibility of current induced magnetization switching for an experimentally realistic parameter set. It is observed that, for the realization of magnetization switching sufficient biased current and moderate field are suitable for the case of low

Gilbert damping. Although, switching can be delayed for large damping, however such system can not be used because the system become highly unstable in such situation, which is unrealistic. It is also to be noted that switching is highly dependent on the strong coupling parameter and it is seen that positive value of that offers more rapid switching than that of negative. It is also seen that switching has a high magnetic configuration dependence. It shows a monotonic increase for both low and high current in very near to parallel configuration. The configuration near anti parallel offers more rapid switching than the parallel. Again, it can also be conclude that the dynamics is highly dependent and controlled by the magnetic field as it becomes of the order of the anisotropy field. As a concluding remark, the results indicate about the switching mechanism in F|S|F spin valve setup for an experimentally favourable parameter set, which may be utilized to bind superconductivity and spintronics [25] together for making practical superconducting-spintronic devices.

#### Acknowledgments

Authors are thankful to Professor Jacob Linder, Department of Physics, Norwegian University of Science and Technology, N-7491 Trondheim, Norway for his very helpful comment during communication, which leads to a considerable improvement of the work.

- 
- [1] S. S. Saxena et al., Nature (London) **406**, 587 (2000).
  - [2] D. Aoki et al., Nature (London) **413**, 613 (2001).
  - [3] C. Pfleiderer et al., Nature (London) **412**, 58 (2001).
  - [4] N. T. Huy et al., Phys. Rev. Lett. **99**, 067006 (2007).
  - [5] J. Flouquet and A. Buzdin, Phys. World **15**, 41 (2002).
  - [6] S. Nandi et al., Phys. Rev. B. **89**, 014512 (2014).
  - [7] A. I. Buzdin, Rev. Mod. Phys. **77**, 935 (2005).
  - [8] Sangjun Oh, D. Youm, and M. R. Beasley, Appl. Phys. Lett. **71**, 2376 (1997).
  - [9] L. R. Tagirov, Phys. Rev. Lett. **83**, 2058 (1999).
  - [10] J. Y. Gu, C.-Y. You, J. S. Jiang, J. Pearson, Ya. B. Bazalia and S. D. Bader, Phys. Rev. Lett. **89**, 267001 (2002).
  - [11] J. Y. Gu, J. A. Cabellero, R. D. Slater, R. Loloee and W. P. Pratt, Jr., Phys. Rev. B **66**, 140507 (2002).
  - [12] F. S. Bergeret, A. F. Volkov, K. B. Efetov, Rev. Mod. Phys. **77**, 1321 (2005).
  - [13] I. C. Moraru, W. P. Pratt, Jr. and Norman O. Birge, Phys. Rev. Lett. **96**, 037004 (2006).
  - [14] J. Zhu, I. N. Krivorotov, K. Halterman and O. T. Valls. Phys. Rev. Lett. **105**, 207002 (2010).
  - [15] P. V. Leksins, et al., Phys. Rev. Lett. **109**, 057005 (2012).
  - [16] N. Banerjee, et al., Nature Communications (London) **5**, 4771 (2014).
  - [17] I. Zutic, J. Fabian and S. Das. Sarma, Rev. Mod. Phys. **76**, 323 (2004).
  - [18] J. C. Slonczewski, J. Magn. Magn. Mater, **159**, L1 (1996).
  - [19] L. Berger, Phys. Rev. B. **54**, 9353 (1996).
  - [20] J. Linder, T. Yokoyama, Phys. Rev. B **83**, 012501 (2011).
  - [21] J. Linder, Phys. Rev. B. **84**, 094404 (2011).
  - [22] A. S. Nunez et al., Phys. Rev. B. **73**, 214426 (2006).
  - [23] X. L. Tang et al., Appl. Phys. Lett. **91**, 122504 (2007).
  - [24] S. Urazhdin and N. Anthony, Phys. Rev. Lett. **99**, 046602 (2007).
  - [25] J. Linder and J. W. A. Robinson, Nature Physics **11**, 307 (2015).
  - [26] X. Waintal and P. W. Brouwer, Phys. Rev. B. **65**, 054407 (2002).
  - [27] S. Takahashi et al., Phys. Rev. Lett. **99**, 057003 (2007).
  - [28] E. Zhao and J. A. Sauls, Phys. Rev. B. **78**, 174511 (2008).
  - [29] V. Braude and Ya. M. Blanter, Phys. Rev. Lett. **100**, 207001 (2008).
  - [30] I. Kulagina and J. Linder, Phys. Rev. B **90**, 054504 (2014).
  - [31] Diana V. Shopova and Dimo I. Uzunov, Phys. Rev. B. **72**, 024531 (2005).
  - [32] E. K. Dahl, A. Sudbo, Phys. Rev. B. **75**, 144504, (2007).
  - [33] D. V. Shopova, T. E. Tsvetkov, D. I. Uzunov, Condens. Matter Phys. **8**, 181 (2005).
  - [34] A. A. Bespalov, A. S. Mel'nikov and A. I. Buzdin, Phys. Rev. B. **89**, 054516 (2014).
  - [35] G. Bastien et al., Phys. Rev. B. **94**, 125110 (2016).
  - [36] T. Akazawa et al., J. Phys.: Condens. Matter **16**, L29 (2004).